3D FINITE-DIFFERENCE TECHNIQUES BASED ON IRREGULAR-GRID FORMULATION: DEVELOPMENT AND TESTING AGAINST KOBE EARTHQUAKE GROUND MOTIONS RECORDED IN OSAKA BASIN

Award No: 1434-HQ-98-GR-00032

Investigators: Arben Pitarka and Robert G. Graves

Wooward-Clyde Federal Services
566 El Dorado Street, Suite 100
Pasadena, CA 91101
tel: (626) 449-7650 / fax: (626) 449-3536 Email: axpitar0@wcc.com

Program Element: II
Key Wors : Develop methodology for modeling 3D wave propagation in sedimentary basins.

INVESTIGATIONS

A common feature of the 3D-FD techniques used in strong ground motion simulations and wave propagation modeling is the use of the uniform-grid formulation (i.e., constant grid spacing), which requires relatively large computer memory. In order to avoid the spatial oversampling introduced by the constant grid-spacing in zones with high velocity we have developed fourth-order expressions for discrete spatial differential operators that can be used in the staggered-grid 3D FD schemes with non-uniform grid spacing to solve the wave equation in 3D elastic media. By applying these operators we are able to partially adapt the grid spacing to the velocity structure in accordance with the accuracy condition required by the finite-difference method. The use of non-uniform grid spacing improves the efficiency of the finite-difference methods when applied to large scale structures.

Finite-difference Operators for the Rectangular Grid With Non-Uniform Spacing

To model wave propagations in 3D elastic media we basically follow the staggered grid finite-difference method proposed by Virieux (1986), Levander (1988), Graves (1996) which solves the following elastodynamic equations:

$$
\begin{aligned}
\partial_t v_x &= b(\partial_x \tau_{xx} + \partial_y \tau_{xy} + \partial_z \tau_{xz}) + f_x \\
\partial_t v_y &= b(\partial_x \tau_{xy} + \partial_y \tau_{yy} + \partial_z \tau_{yz}) + f_y \\
\partial_t v_z &= b(\partial_x \tau_{xz} + \partial_y \tau_{yz} + \partial_z \tau_{zz}) + f_z \\
\\
\partial_t \tau_{xx} &= (\lambda + 2\mu)\partial_x v_x + \lambda(\partial_y v_y + \partial_z v_z) \\
\partial_t \tau_{yy} &= (\lambda + 2\mu)\partial_y v_y + \lambda(\partial_x v_x + \partial_z v_z) \\
\partial_t \tau_{zz} &= (\lambda + 2\mu)\partial_z v_z + \lambda(\partial_x v_x + \partial_y v_y) \\
\partial_t \tau_{xy} &= \mu(\partial_y v_x + \partial_x v_y) \\
\partial_t \tau_{xz} &= \mu(\partial_z v_x + \partial_x v_z) \\
\partial_t \tau_{yz} &= \mu(\partial_z v_y + \partial_y v_z)
\end{aligned}
\qquad (1)
$$

Here, (v_x,v_y,v_z) are the particle velocity components; $(\tau_{xx},\tau_{yy},\tau_{zz},\tau_{xy},\tau_{xz},\tau_{yz})$ are the stress components; (f_x,f_y,f_z) are the body-force components; b is the buoyancy; λ and μ are Lame's coefficients; and $\partial_x,\partial_y,\partial_z$, and ∂_t represent the partial differential operators ∂/∂_x, ∂/∂_y, ∂/∂_z, and ∂/∂_t, respectively. By using second-order approximation for time derivatives, the solution of equations (1) can be expressed in a discrete form by:

$$
\begin{aligned}
v_x^{n+1/2}{}_{i,j,k} &= v_x^{n-1/2}{}_{i,j,k} + \Delta t\, b_x(D_x\tau_{xx} + D_y\tau_{xy} + D_z\tau_{xz})\, |^n{}_{i,j,k} \\
v_y^{n+1/2}{}_{i+1/2,j+1/2,k} &= v_y^{n-1/2}{}_{i+1/2,j+1/2,k} + \Delta t\, b_y(D_x\tau_{xy} + D_y\tau_{yy} + D_z\tau_{yz})\, |^n{}_{i+1/2,j+1/2,k} \\
v_z^{n+1/2}{}_{i+1/2,j,k+1/2} &= v_z^{n-1/2}{}_{i+1/2,j,k+1/2} + \Delta t\, b_z(D_x\tau_{xz} + D_y\tau_{yz} + D_z\tau_{zz})\, |^n{}_{i+1/2,j,k+1/2}
\end{aligned}
$$

$$
\begin{aligned}
\tau_{xx}^{n+1}{}_{i+1/2,j,k} &= \tau_{xx}^{n}{}_{i+1/2,j,k} + \Delta t\,[(\lambda + 2\mu)D_xv_x + \lambda\,(D_yv_y + D_zv_z)]|^{n+1/2}{}_{i+1/2,j,k} \\
\tau_{yy}^{n+1}{}_{i+1/2,j,k} &= \tau_{yy}^{n}{}_{i+1/2,j,k} + \Delta t\,[(\lambda + 2\mu)D_yv_y + \lambda\,(D_xv_x + D_zv_z)]|^{n+1/2}{}_{i+1/2,j,k} \\
\tau_{zz}^{n+1}{}_{i+1/2,j,k} &= \tau_{zz}^{n}{}_{i+1/2,j,k} + \Delta t\,[(\lambda + 2\mu)D_zv_z + \lambda\,(D_xv_x + D_yv_y)]|^{n+1/2}{}_{i+1/2,j,k} \\
\tau_{xy}^{n+1}{}_{i,j+1/2,k} &= \tau_{xy}^{n}{}_{i,j+1/2,k} + \Delta t\,[\mu_{xy}(D_yv_x + D_xv_y)]|^{n+1/2}{}_{i,j+1/2,k} \\
\tau_{xz}^{n+1}{}_{i,j,k+1/2} &= \tau_{xz}^{n}{}_{i,j,k+1/2} + \Delta t\,[\mu_{xz}(D_zv_x + D_xv_z)]|^{n+1/2}{}_{i,j,k+1/2} \\
\tau_{yz}^{n+1}{}_{i+1/2,j+1/2,k+1/2} &= \tau_{yz}^{n}{}_{i+1/2,j+1/2,k+1/2} + \Delta t\,[\mu_{yz}(D_zv_y + D_yv_z)]|^{n+1/2}{}_{i+1/2,j+1/2,k+1/2}
\end{aligned}
\qquad (2)
$$

In these equations, the superscripts refer to the time index, and the subscripts refer to the spatial indices. Δt is the time step and D_x, D_y, D_z represent the central finite-difference operators of the spatial derivatives ∂_x, ∂_y, and ∂_z, respectively.

Suppose that the field variable g represents one component of particle velocity (v_x,v_y,v_z) or stress-tensor $(\tau_{xx},\tau_{yy},\tau_{zz},\tau_{xy},\tau_{xz},\tau_{yz})$. The fourth-order finite-difference operator with respect to x acting on a field variable g can be expressed by the equation

$$D_xg(x,y,z) = c_1g(x+\Delta_1,y,z) + c_2g(x-\Delta_2,y,z) + c_3g(x+\Delta_3,y,z) + c_4g(x-\Delta_4,y,z) \qquad (3)$$

where c_i are four coefficients to be determined. Spatial increments Δ_i can be expressed in terms of the variable grid spacing dx. Similar equations can be used to express the finite-difference operators D_y and D_z.

Since we are considering the spatial derivative of the variable g with respect to x, we assume $g(x,y,z)=g_{yz}\exp(ikx)$ with g_{yz} representing its dependence only on y and z. After replacing g in Eq.3 we obtain:

$$ik = c_1\exp(+ik\Delta_1) + c_2\exp(-ik\Delta_2) + c_3\exp(+ik\Delta_3) + c_4\exp(-ik\Delta_4) \qquad (4)$$

By using the Taylor's expansion up to order $O(\Delta_i^4)$ to approximate the exponentials in Eq. 4 and substituting the obtained equations into Eq. 4 we obtain a system of four linear equations:

$$
\begin{matrix}
1 & 1 & 1 & 1 \\
\Delta_1 & -\Delta_2 & +\Delta_3 & -\Delta_4 \\
-\Delta_1^2 & -\Delta_2^2 & -\Delta_3^2 & -\Delta_4^2 \\
-\Delta_1^3 & +\Delta_2^3 & -\Delta_3^3 & +\Delta_4^3
\end{matrix}
\begin{matrix} c_1 \\ c_2 \\ c_3 \\ c_4 \end{matrix}
=
\begin{matrix} 0 \\ 1 \\ 0 \\ 0 \end{matrix}
\qquad (5)
$$

By solving the system (5) we find the coefficients c_i of the fourth-order finite-difference operator D_x. Coefficients c_i in the operators D_y and D_z are similarly determined.

The coefficients c_i are generated prior to the finite-difference calculation, once the non-uniform grid is chosen, which in turn is based on the velocity distribution and the maximum frequency required in the modeling.

RESULTS

Performance of the Non-Uniform-Grid Finite-Difference Operators

To assess the accuracy of the proposed finite-difference operators, we implemented them into the finite-difference scheme and performed several calculations to model the wave propagation in laterally homogeneous and heterogeneous media. In all tests the synthetic seismograms obtained with the proposed scheme are compared with those obtained with the reflectivity method (REF) or 3D FD technique with constant grid spacing. Here we show results obtained with a flat-layered velocity model and a small basin structure, for a double-couple point source with a focal mechanism of *strike*=30°, *dip*=80°, *rake*=30°.

One of the tests was designed to check the capability of the new scheme to handle the situation where the source is very shallow and embedded into a very soft layer. The source was located at four grid spacings below the free surface at a depth of 0.5 km. Shallow sources are efficient at exciting surface waves in such media.

The velocity model has a soft thin layer at the top of the half-space. The vertical grid spacing increases from the top to depth by a factor of three, the grid spacing in the lower region being 0.375 km. This ratio is proportional to that of shear-wave velocity ratio of the surface layer and the half space. The grid spacing in the upper region and in the two horizontal directions was 0.125 km. The velocity seismograms calculated with the non-uniform FD technique are compared with those obtained with REF at an observation point located on the free surface at the horizontal range of 10 km (Figure 1). The synthetic seismograms are band-pass filtered between 0.1-1.3 Hz. The upper frequency limit was defined assuming a minimum of 6 grid points per shear-wavelength in the vertical direction. The agreement between the two techniques is very good, suggesting that the FD scheme with non-uniform grid spacing can handle models with strong velocity contrast.

Next the analysis were extended to a basin model with a strong velocity contrast between the basin and the bedrock and used a grid spacing which is non-uniform in both horizontal and vertical directions. The semi-ellipsoidal basin, hypocenter and computational region are shown in Figure 2. The 3D grid was divided into two regions with different grid spacings. The grid spacing is 0.1 km in the inner region which includes the basin, and 0.4 km in the outer region. The grid spacing in each of the two regions was defined so as to satisfy the criteria of having 6 grid points per shear-wavelength everywhere in the model. The grid spacing contrast between the two regions replicates the shear-wave velocity contrast between the basin and the bedrock. The region with the refined grid was intentionally extended up to three of the six edges of the model space, including the free surface.

The result of the test is shown in Figure 3, which compares synthetic velocity seismograms calculated with both the constant and varying grid spacings for a double couple point source (*strike*=30°, *dip*=90°, *rake*=30°) , seismic moment $M_o = 10^{25}$ dyne cm and a bell-shaped source-time function with a duration of 0.8 sec. The source is located at a depth of 10 km. The accuracy of the two techniques is expected to be the same in the frequency range 0.1-

1.3 Hz since the smallest grid spacing in the basin is the same in both calculations. The band-pass filtered (0.1-1.3 Hz) velocity seismograms are calculated at receivers located on the free surface along a line across the basin. The synthetics obtained by the two techniques are very close. Because the non-uniform grid calculation required about 6 time less computer core memory than that with the uniform grid and the time increment was the same, the computation time was reduced by a factor of 6. The improvement in computational memory is model-dependent, but for sedimentary basin structures with low velocity the gain is considerable in most cases.

The accuracy of the proposed scheme was assessed also in the cases where the grid spacing varied in the source region. Such cases may be encountered in modeling ground motions for both a double-couple point source or an extended fault. Comparisons between analytical solutions and the new scheme at near-fault stations showed very good agreement between the two techniques. These result also demonstrated that the fault representation by an irregular distribution of point sources with the source spacing smaller than the shortest wavelength does not adversely affect the calculated fault response.

The proposed non-uniform staggered-grid finite-difference formulation is efficient and sufficiently accurate at modeling wave propagations in 3D elastic media. The accuracy and stability conditions are locally the same as in the uniform-staggered-grid scheme. All the numerical tests were performed with a minimum of 6 grid spacings per shortest shear-wavelength. Up to four grid increments did not affect the accuracy of the results.

The work for modeling the ground motion in Osaka Basin from Kobe, Japan earthquake is in progress. Preliminary analysis show that the new technique is capable at handling the very soft surface layer that characterize the surface geology in the Kobe region. In addition to the basin geometry such layer affected significantly the strong ground motion during Kobe earthquake.

References

Graves, R. W. (1996). Simulating seismic wave propagation in 3D elastic media using staggered-grid finite-differences, *Bull. Seism. Soc. Am.* **86**, 1091-1107.

Levander, A. R. (1988). Fourth-order finite-difference P-SV seismograms, *Geophysics* **53,** 1425-1436.

Virieux, J. (1986). P-SV wave propagation in heterogeneous media: velocity-stress finite-difference method, *Geophysics* **51,** 889-901.

REPORTS PUBLISHED

Pitarka, A. (1999), "3D Elastic Finite-Difference Modeling of Seismic Motion Using Staggered Grids With Non-Uniform Spacing", *Bull. Seism. Soc. Am.* (in press).

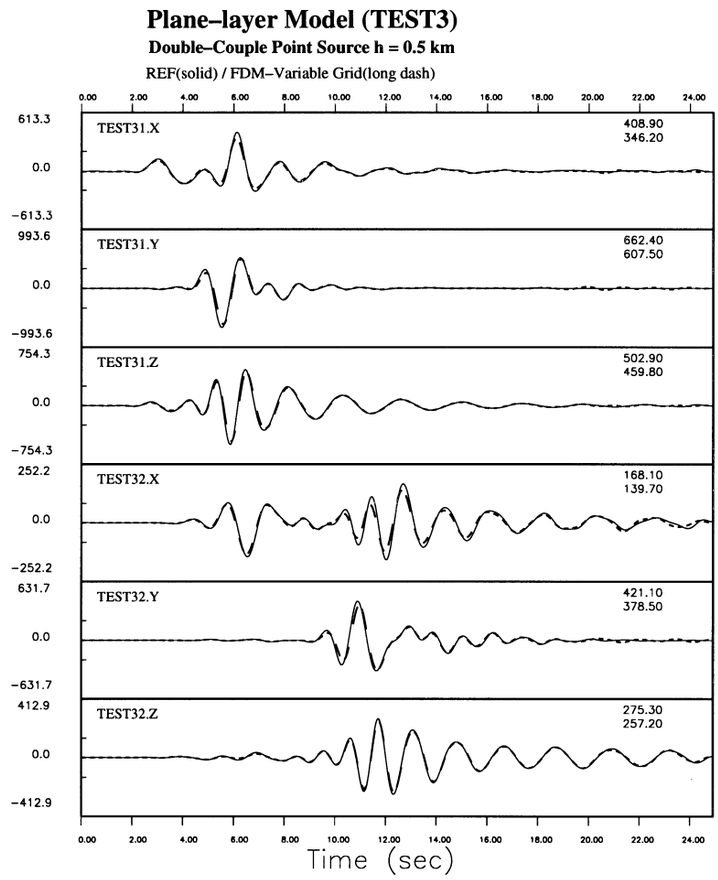

Figure 1. Comparison of three-component synthetic velocity seismograms calculated with the 3D FD method with vertically non-uniform grid spacing (dotted line) and reflectivity method (solid line), for a double-couple point source and a flat-layered velocity model. Peak velocity is indicated on the left of each seismogram.

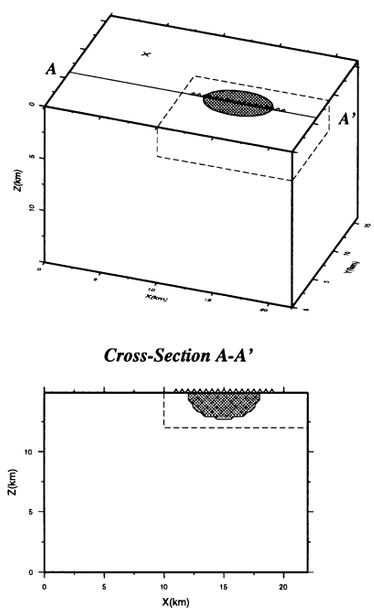

Figure 2. Velocity Model: half-ellipsoid basin structure embedded in a homogeneous half space. The boundary between fine and coarse grid zones is indicated by dotted lines. Triangles indicate the receiver locations and the cross indicates the epicenter location of a double couple at a depth of 10 km.

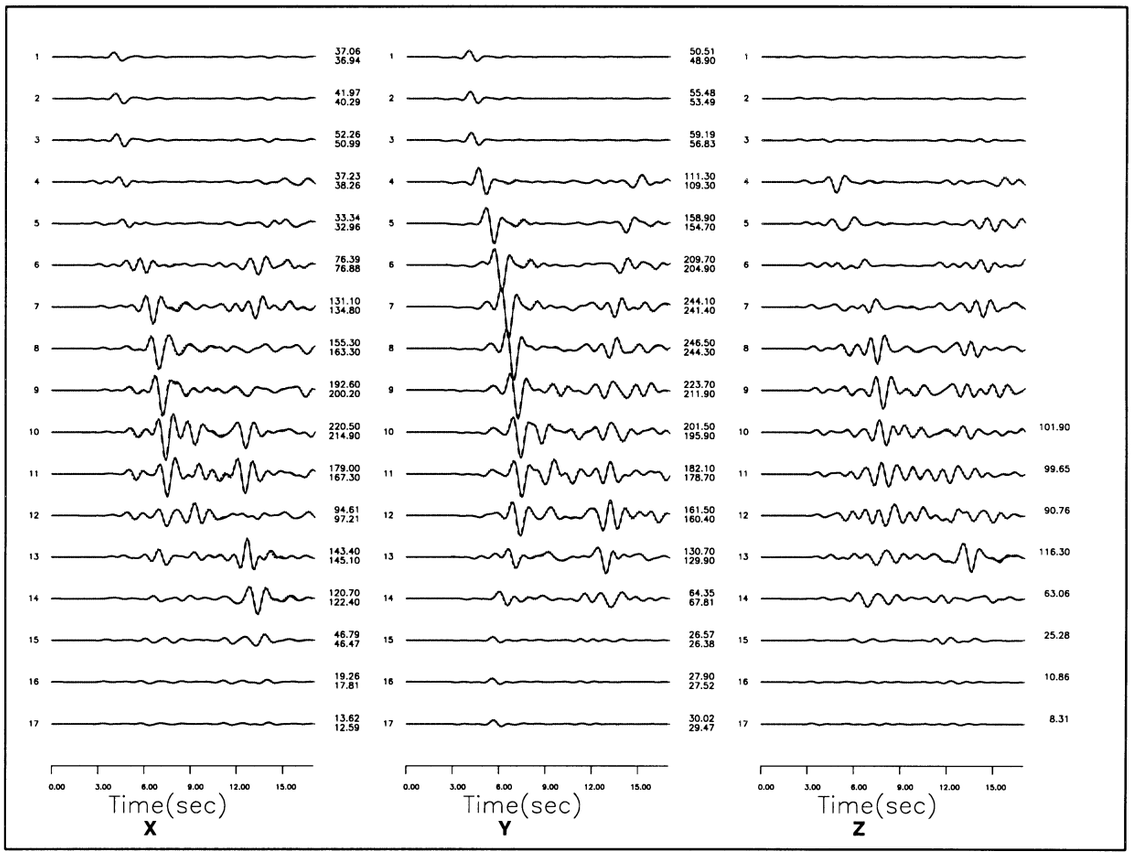

Figure 3. Comparison of three-component velocity seismograms calculated with the non-uniform-grid spacing FD method (dashed trace) and the uniform-grid spacing FD method (solid trace) for the velocity structure shown in Fig.2. All seismograms are band-pass filtered at 0.1-1.3 Hz. Peak velocity is shown on the left of each seismogram.